J Mater Sci: Mater Electron (2015) 26:6843–6847
DOI 10.1007/s10854-015-3299-2

Effects of La^{3+} substitution on structure and temperature dependence of electrical properties of $CaBi_4Ti_4O_{15}$–$Bi_4Ti_3O_{12}$ ceramics

Lingjuan Fei[1,2] · Zhiyong Zhou[1] · Shipeng Hui[1,2] · Xianlin Dong[1]

Received: 25 March 2015 / Accepted: 1 June 2015 / Published online: 13 June 2015

Abstract Structure and temperature dependence of electrical properties of $Ca(Bi,La)_4Ti_4O_{15}$–$(Bi,La)_4Ti_3O_{12}$ (CBT–BIT–xLa) ceramics were studied. With La^{3+} doping content increasing, the samples exhibited diffused dielectric constant anomalies, and the Curie temperature (T_c) decreased. Meanwhile, the dielectric loss of CBT–BIT–xLa was reduced. CBT–BIT–0.8La performed an improved piezoelectric constant (d_{33}) value of 23.4 pC/N and remained until the temperature increased to 500 °C. In addition, CBT–BIT–0.8La performed an enhanced ρ_{dc} value of 3.26×10^{15} Ω cm, at room temperature. CBT–BIT–0.8La showed clearly higher dc resistivity (ρ_{dc}) than CBT–BIT, even with increasing the temperature to 600 °C.

1 Introduction

Piezoelectric materials desired for techniques and devices including piezoelectric sensors should function at high temperatures without failure. Due to their distinctive microstructure, high fatigue resistance, large remnant polarization ($2P_r$) and high Curie temperature (T_c), the intergrowth bismuth layer-structured ferroelectrics (BLSFs) have been given abroad attention for high temperature applications [1–4]. In BLSFs, the high Curie temperature is closely related to Bi^{3+} at A-site with lone pair of $6s^2$ electrons [3–5]. For high temperature vibration sensing applications, the sensitivity of these techniques and devices throughout the temperature ranges is significantly influenced by the temperature dependence of electrical properties including piezoelectric properties and resistivity [6]. However, the temperature stability of BLSFs-based materials is the major problem for applications in electronic devices at high temperature. The piezoelectric constant values of BLSFs are usually less than 20 pC/N and the depoling temperatures could be lower than 400 °C for most of pure intergrowth BLSFs [3, 7, 8]. Piezoelectric materials with high piezoelectric constant usually perform high sensitivity [6, 9]. In addition, high temperature stability of piezoelectric properties is of great help for techniques and devices to retain the same sensitivity throughout the temperature range. However, with the increase of temperature, the dc resistivity of BLSFs would appreciably decrease rapidly. Since the minimum useful frequency of a sensor is inversely proportional to the electrical resistivity, the rapidly decreased resistivity of BLSFs restrains the application of BLSFs in high temperature sensors [6, 10]. These drawbacks of intergrowth BLSFs will restrict their potential applications. Lots of efforts have been paid to improve the electric properties of intergrowth BLSFs. A-site modification and high-valence *B*-site doping have been proven to be effective approaches to improve electric properties of intergrowth BLSFs. Wang et al. reported the substitution of V^{5+} for Ti^{4+} in $SrBi_4Ti_4O_{15}$–$Bi_4Ti_3O_{12}$ (SBT–BIT) could increase $2P_r$ and d_{33} values to 32.5 μC/cm^2 and 18.3 pC/N [8]. Yi et al. [3] have reported La^{3+}-modified Bi_3TiNbO_9–$Bi_4Ti_3O_{12}$ (BTN–BIT) performed an increased piezoelectric constant (d_{33}) value of 16.6 pC/N.

✉ Lingjuan Fei
feilingjuan@126.com

✉ Xianlin Dong
xldong@mail.sic.ac.cn

[1] Key Laboratory of Inorganic Functional Materials and Devices, Shanghai Institute of Ceramics, Chinese Academy of Sciences, Shanghai 201800, China

[2] University of Chinese Academy of Science, Beijing 100049, China

According to the previous report, $CaBi_4Ti_4O_{15}$–$Bi_4Ti_3O_{12}$ (CBT–BIT) performed a high curie temperature (T_c) value of 750 °C, but the dielectric loss is also very high and piezoelectric properties are relatively low [8]. The further information about A- or B-site modification of CBT–BIT intergrowth ceramics is favorable for the improvement in electric properties of CBT–BIT. Meanwhile, the temperature dependence of piezoelectric and dc resistivity properties of A- or B-site modification of CBT–BIT ceramics has not been systematically investigated yet. In the present study, the influences of La^{3+} doping on the temperature dependence of electric properties of CBT–BIT ceramics were studied. The results also show La^{3+} doping leads to a remarkable increase in the piezoelectric properties and dc resistivity properties of CBT–BIT.

2 Experimental procedures

$Ca(Bi,La)_4Ti_4O_{15}$–$(Bi,La)_4Ti_3O_{12}$ ($CaBi_{8-x}La_xTi_7O_{27}$: CBT–BIT–xLa, x = 0, 0.4, 0.8, 0.12) powders were prepared by traditional solid-state reaction method. The stoichiometric mixtures of analytical grade $CaCO_3$, Bi_2O_3, TiO_2 and La_2O_3 were ball-milled and calcined at 850 °C in alumina crucibles for 2 h. The resultant powders were pressed into disks, sintered at 1150 °C for 2 h and cooled naturally. The phase identification and the microstructure characterization were examined on a Rigaku D/max2550 V X-ray diffractometer (XRD) with Cu Kα radiation. Temperature dependent dielectric constant (ε_r) and tan δ was measured by an HP4284A LCR meter. Temperature dependent dc resistivity was measured by a HP4339B high-resistivity meter. The piezoelectric constant (d_{33}) was measured using a ZJ-3A quasi-static d_{33} meter.

3 Results and discussion

Figure 1 shows the XRD patterns of CBT–BIT–xLa ceramics, which represents the enlarged view of the (118) and (201) peaks. The shift in the positions of (118) and (201) peaks for CBT–BIT–xLa is attributed to the addition of La^{3+} in the A sites, and suggests the increase of lattice parameters, which we had discussed in detail elsewhere [11]. Meanwhile, with increasing La^{3+} doping content, the split between the (201) and (021) peaks get weaker and finally disappears when x = 1.2, indicating a structural symmetry transition from orthorhombic to pseudotetragonal.

The variation of dielectric constant (ε_r) of CBT–BIT–xLa ceramics as a function of temperature at 100 kHz is shown in Fig. 2. It can be seen that there are two dielectric peaks at two different temperatures in CBT–BIT–xLa (the lower temperature as T_{m1}, the higher one as T_{m2} or T_c of

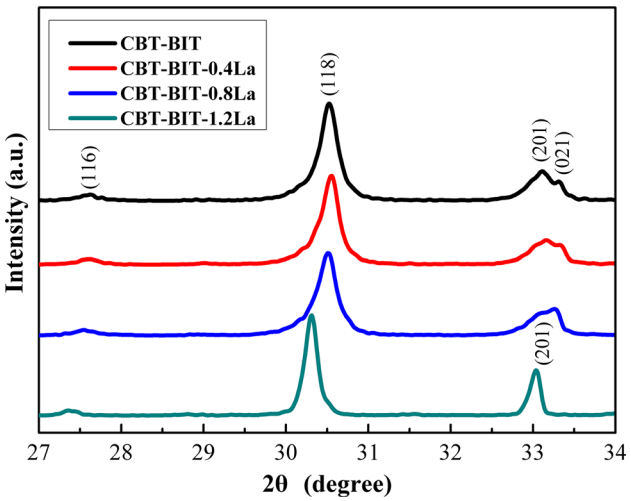

Fig. 1 XRD patterns of CBT–BIT–xLa ceramics (x = 0, 0.4, 0.8, 1.2)

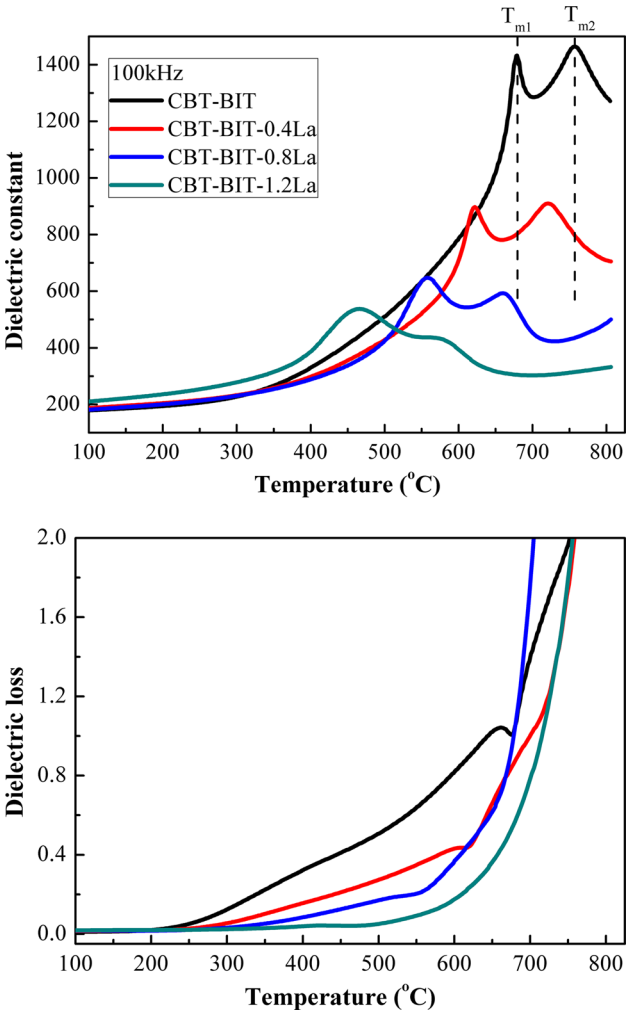

Fig. 2 Temperature dependence of dielectric constant and dielectric loss of CBT–BIT–xLa ceramics at 100 kHz (x = 0, 0.4, 0.8, 1.2)

CBT–BIT) which are related to the phase transition caused by BIT blocks and the phase transition from ferroelectric to paraelectric [8]. The dielectric peaks of CBT–BIT–xLa samples are gradually broadened, and T_{m1} and T_{m2} decrease. Since La^{3+}, Bi^{3+} and Ca^{2+} are randomly distributed on A-site in the structure of CBT–BIT–xLa, the redistribution of A-site cations and the increase of lattice parameters caused by La^{3+} doping may enhance the positional disorder of cations. The cationic disordering could induce random fields, impede the development of long range polar ordering and lead to competition as well as coexistence between long-range and short-range polar order, resulting in the formation of PNRs which have different transition temperatures [4, 12–15], and the broadening of dielectric peaks.

Figure 3 shows the difference between the two dielectric peak temperatures (ΔT: $T_{m1} - T_{m2}$), and the insert shows the variation of T_{m1} and T_{m2} of CBT–BIT–xLa. The T_{m1} and T_{m2} of CBT–BIT are 675 and 750 °C, respectively. With increasing the La^{3+} content, both T_{m1} and T_{m2} decrease, the difference between the two dielectric peak temperatures of CBT–BIT–xLa is increased from 75 °C ($x = 0$) to 106 °C ($x = 1.2$). When $x = 1.2$, $T_{m1} = 466$ °C and $T_{m2} = 571$ °C. It is evident that Bi^{3+} with $6s^2$ lone pair electrons has great influence on the dielectric peak temperature [4]. The substitution of La^{3+} for Bi^{3+} could decrease T_c significantly. However, the dielectric peak around T_{m2} becomes much lower than that around T_{m1}, and the temperature difference between the two peaks in CBT–BIT–xLa becomes bigger with increasing La^{3+} content, which is different from that in BNT–BIT–xLa reported by Yi et al. [16]. That could be caused by the variation of the structure symmetry of CBT–BIT–xLa. With increasing La^{3+} content, CBT–BIT–0.8La and CBT–BIT–1.2La perform a pseudotetragonal–tetragonal phase transition at T_{m2} while CBT–BIT and CBT–BIT–0.4La perform an orthorhombic–tetragonal phase transition.

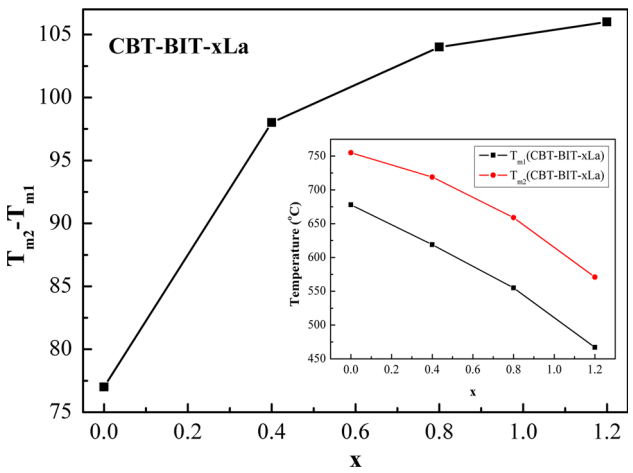

Fig. 3 The difference between the two dielectric peak temperatures (ΔT: $T_{m1} - T_{m2}$), and the *inset*: the variation of T_{m1} and T_{m2} of CBT–BIT–xLa

The dielectric loss of CBT–BIT–xLa decreases with increasing La^{3+} content. The thermal motion of oxygen vacancies caused by the volatilization of Bi_2O_3 can be the predominant reason for the increase of dielectric loss at the temperature range from 100 to 400 °C. And the rapid increase of dielectric loss at higher temperature range can be caused by the movement of ferroelectric domain walls. The substitution of Bi^{3+} by La^{3+} can decrease concentrations of oxygen vacancies and electrons caused by the Bi_2O_3 volatilization, and reduce the dielectric loss caused by the motion of these free charge carriers. The domain wall pinning caused by oxygen vacancies is also reduced.

The dielectric relaxor behavior is further characterized by the modified Curie–Weiss law [17]: $\ln(1/\varepsilon_r - 1/\varepsilon_m) = \gamma \ln(T - T_m) + C$ where ε_m is the value of the dielectric constant at T_{m2}(CBT–BIT) and γ ($1 \leq \gamma \leq 2$) is defined as the degree of diffuseness in ferroelectric–paraelectric transition. For normal ferroelectrics, $\gamma = 1$, while for an ideal relaxor, $\gamma = 2$.

With La^{3+} doping content increasing, the samples exhibit diffused dielectric constant anomalies around T_{m2}. The linear fitting and the value of γ is shown in Fig. 4. It can be seen that the γ value increases when $x \leq 0.8$, gets a maximum value of 1.81 when $x = 0.8$, and then decreases to 1.62. The change of the diffuseness exponent γ symbolizes the variations on the dielectric relaxor behavior of CBT–BIT–xLa and the diffuse phase transition in the structure. In general, the relaxor behavior is closely related to the cationic disordering caused by the different kinds of cations on the same crystallographic site [14, 17–20]. With the content of La^{3+} increasing to 0.8, the cationic disordering may be enhanced, resulting in the increase of diffusion degree of phase transition. However, as we mentioned above, the structure symmetry of CBT–BIT–xLa is also improved. CBT–BIT–1.2La performs a pseudotetragonal–tetragonal phase transition at T_{m2}. The variation of symmetry probably causes a slight suppression of dielectric relaxor behavior and decreased diffuseness exponent.

Temperature dependence of piezoelectric properties of CBT–BIT–xLa ceramics is shown in Fig. 5. With increasing temperature, the CBT–BIT ceramics show excellent resistance to the thermal induced depolarization. The d_{33} value of CBT–BIT ceramics remains 13 pC/N until 670 °C, decreased slightly around 675 °C (T_{m1} of CBT–BIT), and stands great until 720 °C (T_{m2} of CBT–BIT). With the La^{3+} content increasing, the samples show enhanced piezoelectric constants but decreased

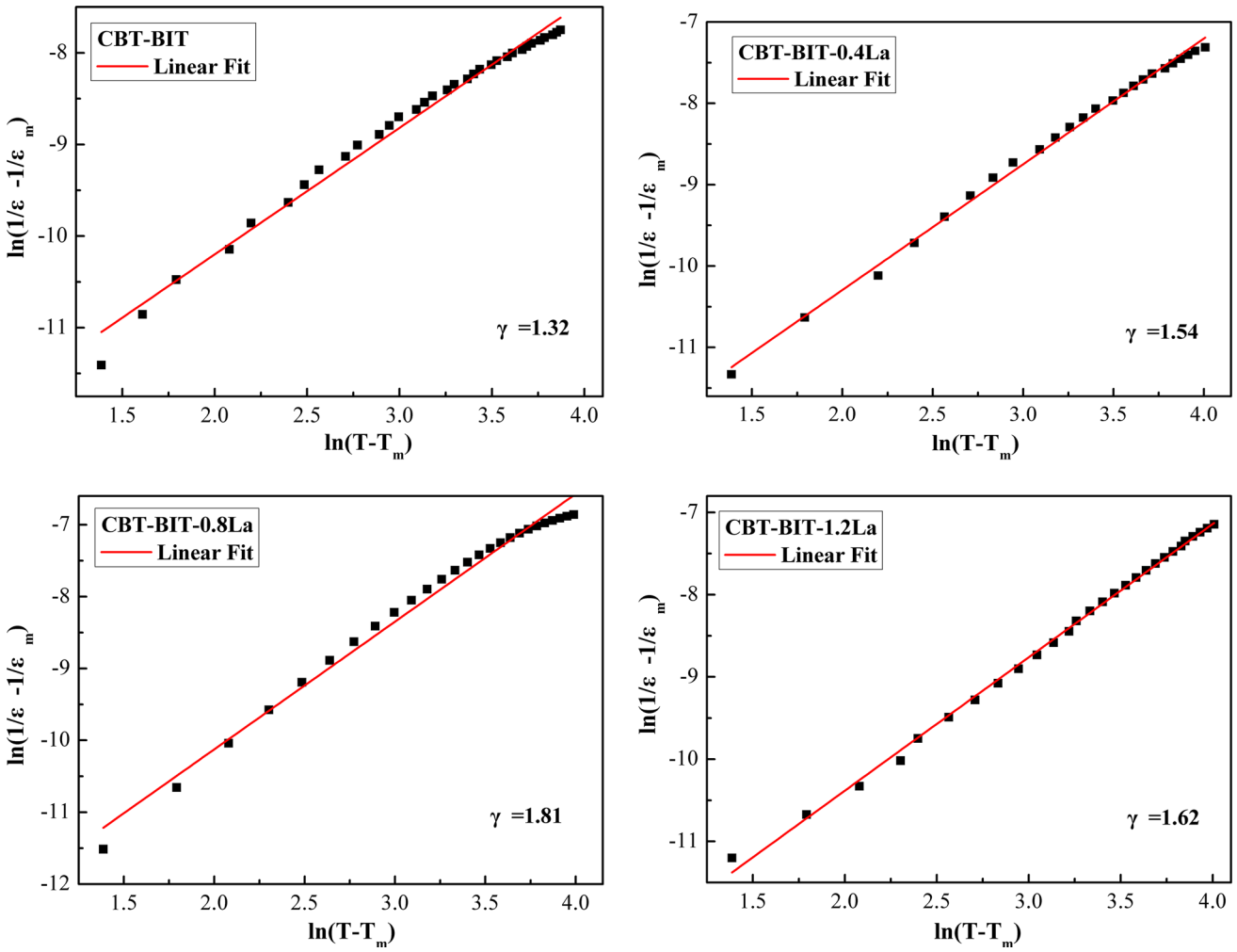

Fig. 4 Plot of $\ln(1/\varepsilon - 1/\varepsilon_m)$ versus $\ln(T - T_m)$ for CBT–BIT–xLa ceramics (x = 0, 0.4, 0.8, 1.2)

depolarization temperatures. The optimal properties are obtained at the composition with x = 0.8, which exhibits piezoelectric constant d_{33} value of 23.4 pC/N and remains 23.4 pC/N until the temperature rises to 500 °C. Compared with the pure CBT–BIT, CBT–BIT–xLa may produce more complicated PNRs with different transition temperatures, because of the heterogeneous distribution of La^{3+} in BIT–xLa part and CBT–xLa part. Therefore, the substitution of La^{3+} for Bi^{3+} could cause the piezoelectric properties of CBT–BIT–xLa thermally unstable well below the Curie point. It could result in significantly decreased phase transition temperatures and the rapid thermal degradation of piezoelectric properties.

Figure 6 shows the temperature dependence of dc resistivity (ρ_{dc}) of CBT–BIT–xLa (x = 0 and 0.8) ceramics. At room temperature, CBT–BIT shows a high ρ_{dc} value of 8.79×10^{13} Ω cm, while CBT–BIT–0.8La performs an

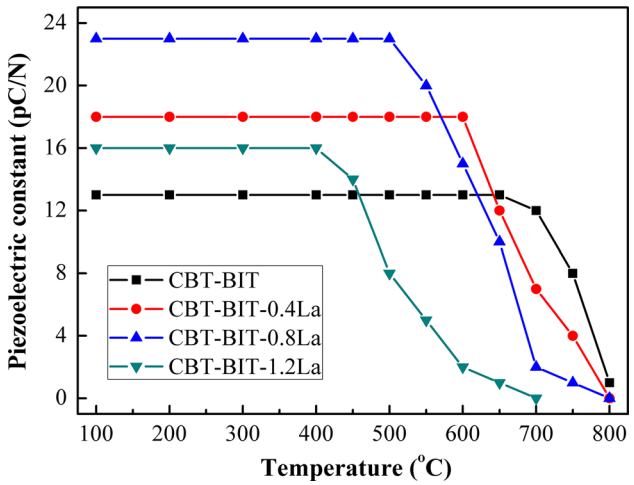

Fig. 5 Temperature dependence of piezoelectric constant of CBT–BIT–xLa (x = 0, 0.4, 0.8, 1.2)

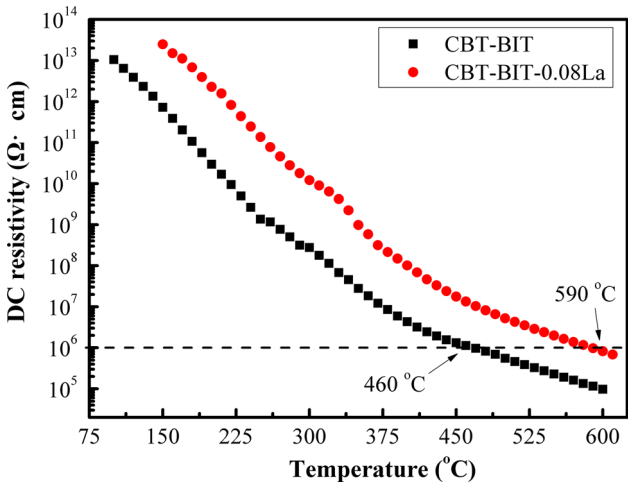

Fig. 6 Temperature dependence of dc resistivity of CBT–BIT–xLa (x = 0, 0.8)

enhanced ρ_{dc} value of 3.26×10^{15} Ω cm. The ρ_{dc} of CBT–BIT–0.8La ceramics has been raised remarkably compared to CBT–BIT ceramics, even when the temperature rises to 600 °C. This is probably attributed to decreased concentrations of free charge carriers. The motion of oxygen vacancies and free electrons plays an important role in the variation of ρ_{dc} of intergrowth BLSFs in the temperature range from 75 to 600 °C [21, 22]. As reported before, the bond strength of La–O is stronger than that of Bi–O [23, 24]. La^{3+} doping can decrease the concentration of oxygen vacancies and electrons which is likely to be caused by the volatilization of Bi_2O_3. The high resistivity is beneficial to piezoelectric applications of intergrowth BLSFs at high temperature.

4 Conclusions

Structure and temperature stability of electric properties of CBT–BIT–xLa ceramics were studied. A phase transition from orthorhombic to pseudotetragonal was observed by XRD analysis when $x \geq 0.8$. With increasing x, the samples exhibited diffused dielectric constant anomalies. Meanwhile, due to La^{3+} doping, the dielectric loss of CBT–BIT–xLa was reduced. CBT–BIT–xLa performed an enhanced d_{33} value of 23.4 pC/N when $x = 0.8$ and remained until the temperature increased to 500 °C. At room temperature, CBT–BIT shows a high ρ_{dc} value of 8.79×10^{13} Ω cm, while CBT–BIT–0.8La performs an enhanced ρ_{dc} value of 3.26×10^{15} Ω cm. Moreover, CBT–BIT–0.8La also performed clearly (about ten times) higher ρ_{dc} than CBT–BIT, even at high temperature.

Acknowledgments The authors acknowledge the financial support by the National Natural Science Foundation of China (Grant No. 11304334).

References

1. T. Wei, C.Z. Zhao, C.P. Li, Y.B. Lin, X. Yang, H.G. Tan, J. Alloy Compd. **577**, 728–733 (2013)
2. T. Wei, C.P. Li, Q.J. Zhou, Y.L. Zou, L.S. Zhang, Mater. Lett. **118**, 92–95 (2014)
3. Z.G. Yi, Y.X. Li, Y. Liu, Phys. Status Solidi A **208**, 1035–1040 (2011)
4. Z.G. Yi, Y.X. Li, J.T. Zeng, Q.B. Yang, D. Wang, Y.Q. Lu, Q.R. Yin, Appl. Phys. Lett. **87**, 202901 (2005)
5. T. Sivakumar, M. Itoh, Eur. J. Inorg. Chem. **2011**, 5343–5346 (2011)
6. S.J. Zhang, F.P. Yu, J. Am. Ceram. Soc. **94**, 3153 (2011)
7. H. Zhang, H. Yan, M.J. Reece, J. Appl. Phys. **107**, 104111 (2010)
8. W. Wang, D. Shan, J.B. Sun, X.Y. Mao, X.B. Chen, J. Appl. Phys. **103**, 044102 (2008)
9. K. Kim, S.J. Zhang, G. Salazar, X.N. Jiang, Sensor. Actuat. A Phys. **178**, 40 (2012)
10. R.C. Turner, P.A. Fuierer, R.E. Newnham, T.R. Shrout, Appl. Acoust. **41**, 299 (1994)
11. L.J. Fei, Z.Y. Zhou, S.P. Hui, X.L. Dong, Y.S. Li, Mater. Lett. **156**, 165 (2015)
12. P.Y. Fang, H.Q. Fan, J. Li, F. Liang, J. Appl. Phys. **107**, 064104 (2010)
13. J. Zhu, X.B. Chen, J.H. He, J.C. Shen, J. Solid State Chem. **178**, 2832–2837 (2005)
14. C. Karthik, N. Ravishankar, M. Maglione, R. Vondermuhll, J. Etourneau, K.B.R. Varma, Solid State Commun. **139**, 268 (2006)
15. Y. Liu, R.L. Withers, X.Y. Wei, J.D. Fitz, Gerald. J. Solid State Chem. **180**, 858 (2007)
16. Z.G. Yi, Y.X. Li, Y. Wang, Q.R. Yin, Appl. Phys. Lett. **88**, 152909 (2006)
17. C.L. Diao, J.B. Xu, H.W. Zheng, L. Fang, Y.Z. Gu, W.F. Zhang, Ceram. Int. **39**, 6991–6995 (2013)
18. B.R. Kannan, B.H. Venkataraman, Ceram. Int. **40**, 16365–16369 (2014)
19. C.L. Diao, H.W. Zheng, Y.G. Zhang, Z. Chen, L. Fang, Ceram. Int. **40**, 13827–13832 (2014)
20. H. Li, Q. Meng, D. Gong, H. Tian, Z. Zhou, J. Eur. Ceram. Soc. **34**, 4185–4192 (2014)
21. Z.G. Yi, Y.X. Li, Z.Y. Wen, S.R. Wang, J.T. Zeng, Q.R. Yin, Appl. Phys. Lett. **86**, 192906 (2005)
22. Z.G. Yi, Y.X. Li, Y. Wang, Q.R. Yin, Appl. Phys. Lett. **88**, 162908 (2006)
23. M. Roy, I. Bala, S.K. Barbar, S. Jangid, P. Dave, J. Phys. Chem. Solids **72**, 1347–1353 (2011)
24. Z.G. Yi, Y.X. Li, Q.B. Yang, Q.R. Yin, Ceram. Int. **34**, 735–739 (2008)